Activity-controlled clogging and unclogging of micro-channels

L. Caprini[1], F. Cecconi[2], C. Maggi[2], and U. Marini Bettolo Marconi[3]
[1] *Gran Sasso Science Institute (GSSI), Via. F. Crispi 7, 67100 L'Aquila, Italy.*
[2] *Istituto dei Sistemi Complessi - CNR and Dipartimento di Fisica, Università di Roma Sapienza, P.le Aldo Moro 2, 00185, Rome, Italy*
[3] *Scuola di Scienze e Tecnologie, Università di Camerino - via Madonna delle Carceri, 62032, Camerino, Italy.*

(Dated: July 23, 2020)

We propose a mechanism to control the formation of stable obstructions in two-dimensional micro-channels of variable sections taking advantage of the peculiar clustering property of active systems. Under the activation of the self-propulsion by external stimuli, the system behaves as a switch according to the following principle: by turning-on the self-propulsion the particles become active and even at very low densities stick to the walls and form growing layers eventually blocking the channel bottleneck, while the obstruction dissolves when the self-propulsion is turned off. We construct the phase diagram distinguishing clogged and open states in terms of density and bottleneck width. The study of the average clogging time, as a function of density and bottleneck width, reveals the marked efficiency of the active clogging that swiftly responds to the self-propulsion turning on. The resulting picture shows a profound difference with respect to the clogging obtained through the slow diffusive dynamics of attractive passive Brownian disks. This numerical work suggests a novel method to use particles with externally tunable self-propulsion to create or destroy plugs in micro-channels.

Several technological and industrial processes require the control of fluid flows through channels and pores at mesoscopic scales. In this context, it is important to find strategies either favoring or preventing the sudden blockage (clogging) of the channels by particle aggregates and cohesive matter [1]. Recently, materials that spontaneously respond to environmental changes, known as smart materials, seem to offer new opportunities for a clever solution to this kind of problem. Smart materials can also be used to deliver cohesive substances into specific regions in order to reinforce surfaces and repair fractures or damages [2, 3]. In principle, the material aggregation could be used to form obstructions capable of blocking the passage of undesirable debris or harmful chemical and biological agents. In this Letter, we provide a proof of concept that self-propelled particles [4–7], whose active force can be controlled by external inputs [8], can be employed as smart materials able to generate removable obstructions into channels by aggregation. Indeed, it has been recently shown that genetically engineered *E. Coli* bacteria [9–11] and certain Janus particles [8, 12–14] can be externally controlled by a light stimulus and their activity can be rapidly switched on/off by modulating the illumination power. Specifically, we suggest taking advantage of the self-propelled particle propensity to spontaneously form stable aggregates and undergo motility induced phase separation (MIPS) [15–19], as experimentally observed for artificial microswimmers [8, 16, 20–23] or bacteria [24–26] and reproduced by numerical simulations [27–38].

Our mechanism based on the clustering of active particles is able to work as a switch to clog/unclog channels by turning on/off the self-propulsion. Its usefulness is also suggested by the low particle concentrations required. In fact, the cluster formation is strongly enhanced by the presence of confining geometries, as experimentally shown for bacteria [39–41] or artificial microswimmers [13, 42], since active particles accumulate near boundaries [43–46], wall channels [47–51], and obstacles [52–55]. The employment of active particles, instead of passive colloidal particles, to control the channel occlusion leads to further advantages. Passive particles cluster only in the presence of attractive interactions and the addition of depletants [56, 57] but, even in these cases, exhibit a very slow dynamics. As a consequence, the clogging formation is very slow and has been experimentally and numerically observed only when accelerating the access of passive particles into the channel, for instance, by imposing external fluid flows [58–61]. By contrast, as we shall see, active particles block the channel in a much shorter time than passive colloids, revealing their prominent efficiency. This property is crucial in view of the possibility of achieving efficient switching-like behaviors to clog/unclog channels.

We consider a system of N interacting self-propelled disks in two dimensions. According to the Active Brownian Particles (ABP) dynamics [62, 63], the self-propulsion is modeled as a time-dependent force with fixed modulus, v_0, and orientation, $\mathbf{n}_i = (\cos\theta_i, \sin\theta_i)$, where the angles, θ_i, evolve as independent Wiener processes. The dynamics of the particle positions, $\mathbf{x}_i$, is governed by

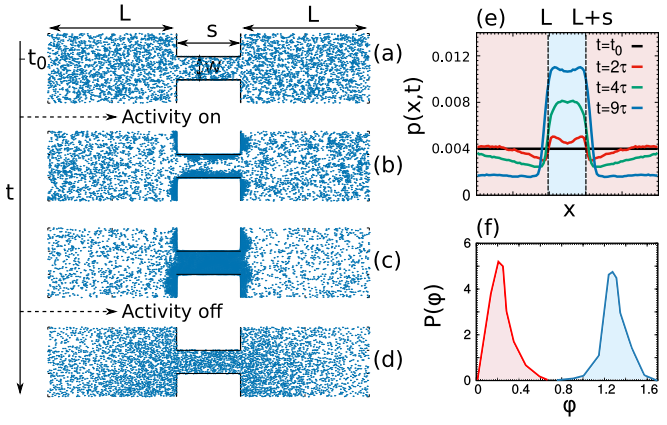

Figure 1. Phenomenology of the clogging process. Panels (a)-(d) show the snapshots of the typical time evolution of the system, with $w = 20$, $\rho = 0.3$, $D_r = 1$, $v_0 = 25$. In particular, panel (a) reports the starting homogeneous configuration in the absence of self-propulsion. Panel (b) and (c) are obtained before and after the plug formation after the active force is turned on. Finally, in panel (d), we report a configuration relaxing towards the homogeneous state since the active force is turned off. In panel (e), we study the particle density, $p(x,t)$, for different times, where the light blue and the pink regions mark the bottleneck and the lateral boxes, respectively. Panel (f) shows the stationary distribution of the packing fraction, $P(\phi)$, calculated in the bottleneck (blue curve) and in the lateral boxes (red curve) for the parameter setting of the other panels.

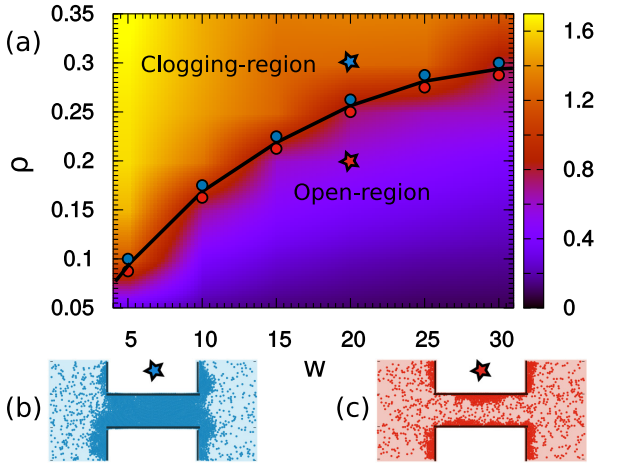

Figure 2. Clogging phase diagram. Panel (a): phase diagram as a function of bottleneck width, w, and density of the system, ρ. Colors represent the steady-state density values in the bottleneck, $\langle \rho_b \rangle$. The solid black curve indicates the clogging-line numerically obtained, separating clogged from open states. Blue and red circles mark the lowest and the highest values of ρ at which clogged and open states are still observed. Panels (b) and (c) report two zooms of the bottleneck occupation above and below the clogging line, in correspondence of the colored stars in the phase diagram. Simulations are run with $D_r = 1$, $v_0 = 25$, $L = 100$, $H = 60$ and $s = 50$.

overdamped stochastic equations:

$$\gamma \dot{\mathbf{x}}_i = \mathbf{F}_i + \mathbf{F}_i^w + \gamma v_0 \mathbf{n}_i \tag{1a}$$

$$\dot{\theta}_i = \sqrt{2D_r}\xi_i \,, \tag{1b}$$

where ξ_i is a white noise with unit variance and zero average. The constants γ and D_r denote the friction and the rotational diffusion coefficients, respectively, and, in particular, the latter determines the typical persistence time of the active force, $\tau = 1/D_r$. The first force term, $\mathbf{F}_i = -\nabla_i U_{tot}$, models the steric repulsion between two disks, where $U_{tot} = \sum_{i<j} U(|\mathbf{r}_{ij}|)$ with $\mathbf{r}_{ij} = \mathbf{x}_i - \mathbf{x}_j$ and the shape of U is chosen as a truncated and shifted Lennard-Jones potential, $U(r) = 4\epsilon[(\sigma/r)^{12} - (\sigma/r)^6] + \epsilon$ for $r \leq 2^{1/6}\sigma$ and zero otherwise. The constants σ and ϵ represent the particle diameter and the energy scale of the interactions, respectively. The term, $\mathbf{F}_i^w$, is the repulsion exerted by the rigid boundaries, modeled as soft reflecting walls, derived by the potential, $V(k(x) - y)$, where the curve $y = k(x)$ is the wall profile. Explicitly, this force is $\mathbf{F}_i^w = -V'(k(x) - y)\hat{\mathbf{n}}$, being $\hat{\mathbf{n}}$ the normal direction with respect to $y = k(x)$, such that any tangential or torque contributions exerted by the boundaries are neglected. Further details about the implementation of the boundaries are reported in Sec. 1 of the Supplemental Material (SM). The system consists of two boxes of area $L \times H$ connected by a bottleneck of size $s \times w$, as schematically illustrated in Fig. 1 (a): the solid black lines define the bottleneck region, while periodic boundary conditions are applied to the rest of the channel.

We study the dynamics (1) at fixed active force by varying the density, ρ, and the bottleneck width, w. Simulations started from homogeneous configurations, in the absence of active forces, Fig. 1 (a). At the initial time t_0, we turn on the self-propulsion and let the system evolve for a final time, $T = 10^2/D_r$. A typical time evolution, at $\rho = 0.3$ and $w = 20$, is schematically illustrated in panels (b), (c) and (d). In a first transient regime, particles accumulate in front of the bottleneck walls forming two symmetric growing layers, Fig. 1 (b). Subsequently, the two layers coalesce and clog the bottleneck, Fig. 1 (c), forming a very dense and cohesive cluster as revealed by the bimodal shape of the density distribution, Fig. 1 (f). Finally, the plug dissolves when the active force is switched off and the system gradually recovers a homogeneous configuration, Fig. 1 (d). The scenario described by panels (a)-(d) is quantitatively confirmed by the plot of the time-dependent density distribution, $p(x,t)$, along the channel, at different times, Fig. 1 (e). Thus, by turning the self-propulsion on/off, the system in practice behaves as a switch to clog and unclog the channel. However, for w or ρ values small enough, the system is not able to attain a steady-state with stable bottleneck obstructions as reported in Fig. 2 (c) where the steady-state is characterized by small clusters of particles close

to the bottleneck walls (open state).

The distinction between clogged and open states can be achieved by computing the average density in the bottleneck region, $\langle\rho_b\rangle$, after the ρ-trajectories have reached their plateau. A close inspection of the configurations allows us to verify that clogged states are those with $\langle\rho_b\rangle \gtrsim 1$, while open states correspond to $\langle\rho_b\rangle \lesssim 1$. Through this heuristic criterion, we construct the phase diagram of the system as a function of ρ and w, Fig. 2 (a), where clogged and open configurations are separated by a solid black line (clogging-line). The clogging-line displays a monotonic growth with both ρ and w almost saturating around $\rho = 0.3$, which is well below the critical ρ-value to observe the MIPS-transition in the confinement-free system [64–67]. The color-map encodes the values of $\langle\rho_b\rangle$ in the bottleneck region showing that a sharp color variation occurs in the proximity of the clogging line and, in the clogged states, plugs become less cohesive as w grows. We remark that the clogged states are obtained even at very small densities constituting a strong advantage in the potential applicability of our mechanism to real devices.

To work as a switching mechanism, the clogging process needs to be sufficiently swift in the response to the turning on of the active force. In this respect, we monitor the time behavior of the local density in the bottleneck, $\rho_b(t)$. Figs. 3 (a)-(b) illustrate the typical dynamics of the clogging process for a bottleneck of width $w = 10$. In particular, panel (a) compares the single fluctuating trajectory of $\rho_b(t)$ with its ensemble average $\langle\rho_b(t)\rangle$ for two different values of ρ. All the curves saturate at a plateau whose value indicates the clogging degree of the stationary state. Specifically, the higher and lower values correspond to clogged (green curves) and open states (red curves), respectively. In addition, the former are self-averaging while the latter are still characterized by more fluctuating behaviors, even in the steady-state configurations, since the layers of particles attached to the walls reorganize without merging. The dashed lines in Fig. (3) (a) represent the theoretical predictions of $\langle\rho_b(t)\rangle$

$$\langle\rho_b(t)\rangle = \frac{\langle\rho_b\rangle\rho}{\rho + (\langle\rho_b\rangle - \rho)\, e^{-t/\alpha}}\,, \qquad (2)$$

where α is a fitting parameter. Eq. (2) is the solution of the logistic equation which, for the present system, is derived in Sec. 3 of the SM under suitable approximations, observing that the increase of $\langle\rho_b(t)\rangle$ is mainly determined by the particles approaching almost *ballistically* the bottleneck and that the probability to remain trapped is roughly proportional to $\rho_b(t)$. The prediction (2) reveals also a good agreement with the numerical results for $\langle\rho_b(t)\rangle$ as shown in Fig. 3 (b) for several values of ρ giving rise to clogged configurations. In these cases, $\langle\rho_b(t)\rangle$ saturates at a common plateau that is determined by the maximum packing density in the bottleneck.

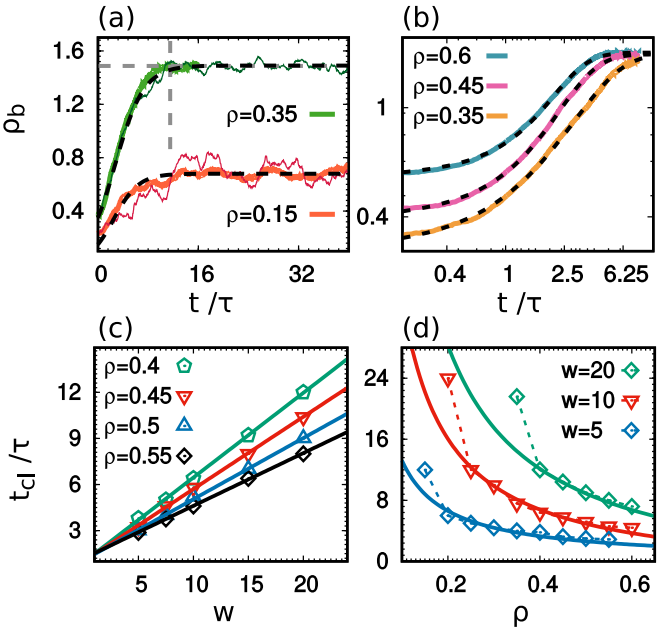

Figure 3. Dynamics of the plug formation. Panels (a) and (b) plot the time evolution of the density in the bottleneck, $\rho_b(t)$, for $w = 10$. Panel (a) shows single-trajectories (thin lines) and the ensemble average, $\langle\rho_b(t)\rangle$ (tick lines), taken over 20 independent initial configurations. The dashed grey horizontal line marks the asymptotic value $\langle\rho_b\rangle$, while the dashed vertical line indicates the time at which the asymptotics is reached. Panel (b) plots $\langle\rho_b\rangle$ as a function of t/τ for three different values of ρ leading to clogging configurations. Both in panels (a) and (b), dashed black lines are obtained by a fit to data with Eq. (2). Panel (c) contains the clogging time $t_{\rm cl}$ as a function of w for different values of ρ, where solid lines are obtained from numerical linear fits. Panel (d) reports $t_{\rm cl}$ vs ρ for different values of w. Points are obtained from simulations, solid lines from Eq. (3) and dotted lines are just eye-guides. Simulations are performed with $\tau = 1/D_r = 1$, $v_0 = 25$, $L = 100$, $H = 60$ and $s = 50$.

The temporal delay of the switch can be estimated as the time, $t_{\rm cl}$, needed to observe the plug formation in the channel (clogging time). Operatively, $t_{\rm cl}$ is measured as the time such that $\langle\rho_b(t)\rangle$ attains the asymptotic value $\langle\rho_b\rangle$ with an uncertainty of 5%. To characterize the switching efficiency, we study the dependence of $t_{\rm cl}$ on the bottleneck width w and density ρ. Fig. 3 (c) shows the linear scaling of $t_{\rm cl}$ as a function of w for different values of ρ (straight lines are linear fits to data). Instead, Fig. 3 (d) reports the monotonic decrease of $t_{\rm cl}$ with ρ, showing that for low values of ρ the onset of the clogging state is prohibitive in time. However, in view of the possible applications, it is encouraging that there exists an extensive range of w and ρ where $t_{\rm cl}$ is only of the order of a few persistence times, τ, of the self-propulsion. An analytical prediction of $t_{\rm cl}$ can be obtained upon the assumption that the plug formation very weakly affects

the bulk average density (large lateral boxes):

$$t_{\rm cl} \approx \frac{sw}{\mathcal{R}} \frac{D_r}{2v_0^2} \left(\frac{\langle \rho_b \rangle}{\rho} - 1 \right) , \qquad (3)$$

where $\mathcal{R}$ is a geometrical factor (see Sec. 1 of the SM). The comparison with data in Fig. 3 (d) reveals a good agreement except for the range of low values of ρ, where Eq. (3) underestimates $t_{\rm cl}$ because the hypothesis of almost constant bulk-density is no longer applicable.

The above results are very promising from a practical perspective to design real switching devices based on the active clogging. One can argue that the same process could be obtained through the coarsening of passive attractive colloids upon the introduction of wall-attractive interactions via chemical coating of the bottleneck walls. This possibility can be tested by replacing active with attractive passive particles in the presence of attractive bottleneck walls (Sec. 4 of the SM). However, our simulations do not show any bottleneck obstruction within the typical times taken by the active system to approach the clogged state. Indeed, the simple self-diffusion alone constitutes a very slow transport mechanism, as supported by direct simulations (Sec. 6 of the SM), where a system of independent passive particles escape a box across two lateral holes, mimicking the presence of the bottleneck. To get a qualitative idea of the $t_{\rm cl}$-scaling with the bottleneck width in the passive clogging process, we resort to Monte Carlo simulations of an equilibrium attractive lattice gas within the channel considered so far. Sec. 5 of the SM shows the scaling $t_w \propto w^2$ independently of the temperature that, in comparison with the linear scaling of the active $t_{\rm cl}$, corroborates the idea that the formation of plugs in passive systems is less efficient. As a conclusion, passive colloids cannot be considered as good candidates for the implementation of switches similar to those suggested in this work.

To understand the dynamical properties of the plug, we study the typical configuration of a clogged bottleneck, see Fig. 4 (a), where the particles are colored according to the orientations of their self-propulsions, θ_i. Since the angles θ_i's evolve independently (Eq. (1b)), colors are randomly distributed in the whole system. However, the particle velocities, $\mathbf{v}_i = \dot{\mathbf{x}}_i$, tend to spontaneously align each other, revealing the emergence of large aligned domains [27, 28], whose particles have a common velocity orientation, β_i, with respect to the $\hat{\mathbf{x}}$-axis (Fig. 4 (b)). Near the bottleneck boundaries, the orientations become preferentially parallel to the walls, as revealed by the symmetric peaks in $(0, \pi)$ of the steady-state distribution $P(\beta)$, Fig. 4 (c). Moving towards the middle of the bottleneck, the peaks broaden as shown in Fig. 4 (c) for two sections placed at the wall and the middle of the bottleneck (for comparison we report also the $P(\beta)$ in the bulk of the lateral boxes, which is completely flat due to the absence of preferential orientations). Fig. 4 (d) compares the distribution of the single-particle velocity modulus in the bottleneck and lateral boxes. In the latter case, the distribution is peaked around v_0, coinciding with the velocity modulus of a free independent self-propelled particle. Instead, in the bottleneck, the distribution is peaked at a value of $|\mathbf{v}| \ll v_0$, since, despite the alignment mechanism, the particles move slowly and this guarantees the stability of the obstruction.

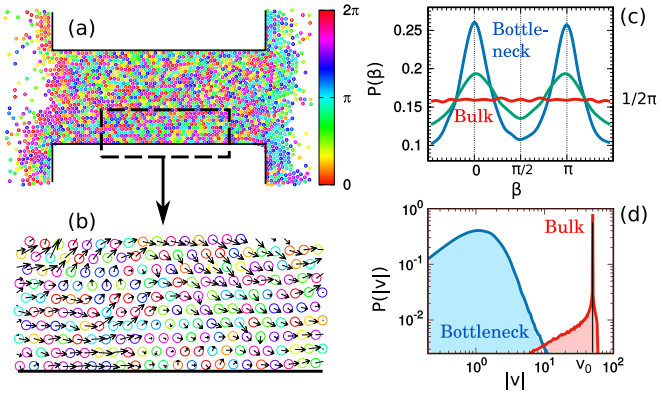

Figure 4. Panel (a) illustrates a snapshot configuration realized with $w = 20$ and $\rho = 0.3$ at time $T = 50\tau$, while panel (b) is a zoom of the area delimited by the dashed black line in panel (a). Colors encode the orientations of the self-propulsions with respect to the $\hat{\mathbf{x}}$-axis, while black arrows represent the velocity vectors. Panel (c) shows $P(\beta)$, the steady-state distributions of the velocity orientation. The blue distribution is in a small layer of width $H/5$ attached to the walls while the green one in a layer of width $H/5$ placed at the center of the bottleneck. Finally, the red $P(\beta)$ is given by averaging the velocity in a square region in the bulk of the lateral boxes. In panel (d), we report $P(|\mathbf{v}|)$, i.e. the steady-state distribution of the velocity modulus, where blue and red curves are obtained averaging the velocities in the bottleneck and bulk regions of the lateral boxes. Simulations are run with $D_r = 1$, $v_0 = 25$, $L = 100$, $H = 60$ and $s = 50$.

In conclusion, we have presented a mechanism to control the plug formation in channels by turning on/off the self-propulsion. The working principle relies on the spontaneous formation of particle clusters preferentially near the walls. The advantage of the method is the rapidity of the plug formation, even using very small densities of self-propelled particles. This controlled clogging could be in practice achieved by exploiting the light-sensitivity of certain self-propelled particles, such as Janus colloids or genetically engineered *E. Coli* bacteria. Furthermore, we expect the switching-mechanism to be more efficient in experimental devices than our simulated systems since Janus particles usually make clustering at smaller densities with respect to numerical simulations [8]. In addition, a proper design of wall geometries [68–72] or the introduction of pillars in the bottleneck region [73] can optimize the clogging process taking advantage of enhanced trapping mechanisms [71, 74–76].

[1] E. Dressaire and A. Sauret, Soft Matter **13**, 37 (2017).
[2] R. Van der Sman, Soft Matter **5**, 4376 (2009).
[3] W. Zhang, X. Tang, N. Weisbrod, and Z. Guan, Journal of Mountain Science **9**, 770 (2012).
[4] M. C. Marchetti, J. F. Joanny, S. Ramaswamy, T. B. Liverpool, J. Prost, M. Rao, and R. A. Simha, Rev. Mod. Phys. **85**, 1143 (2013).
[5] C. Bechinger, R. Di Leonardo, H. Löwen, C. Reichhardt, G. Volpe, and G. Volpe, Reviews of Modern Physics **88**, 045006 (2016).
[6] L. Berthier, E. Flenner, and G. Szamel, The Journal of chemical physics **150**, 200901 (2019).
[7] G. Gompper, R. G. Winkler, T. Speck, A. Solon, C. Nardini, F. Peruani, H. Löwen, R. Golestanian, U. B. Kaupp, L. Alvarez, *et al.*, Journal of Physics: Condensed Matter **32**, 193001 (2020).
[8] J. Palacci, S. Sacanna, A. Steinberg, D. Pine, and P. Chaikin, Science , 1230020 (2013).
[9] J. M. Walter, D. Greenfield, C. Bustamante, and J. Liphardt, Proceedings of the National Academy of Sciences **104**, 2408 (2007).
[10] J. Arlt, V. A. Martinez, A. Dawson, T. Pilizota, and W. C. Poon, Nature communications **9**, 1 (2018).
[11] G. Frangipane, D. Dell'Arciprete, S. Petracchini, C. Maggi, F. Saglimbeni, S. Bianchi, G. Vizsnyiczai, M. L. Bernardini, and R. Di Leonardo, Elife **7**, e36608 (2018).
[12] I. Buttinoni, G. Volpe, F. Kümmel, G. Volpe, and C. Bechinger, Journal of Physics: Condensed Matter **24**, 284129 (2012).
[13] G. Volpe, I. Buttinoni, D. Vogt, H.-J. Kümmerer, and C. Bechinger, Soft Matter **7**, 8810 (2011).
[14] F. Schmidt, B. Liebchen, H. Löwen, and G. Volpe, The Journal of chemical physics **150**, 094905 (2019).
[15] M. E. Cates and J. Tailleur, Annu. Rev. Condens. Matter Phys. **6**, 219 (2015).
[16] J. Bialké, T. Speck, and H. Löwen, J. Non-Cryst. Solids **407**, 367 (2015).
[17] Z. Ma, M. Yang, and R. Ni, arXiv preprint arXiv:2004.02376 (2020).
[18] Y. Fily and M. C. Marchetti, Phys. Rev. Lett. **108**, 235702 (2012).
[19] G. Gonnella, D. Marenduzzo, A. Suma, and A. Tiribocchi, C. R. Phys. **16**, 316 (2015).
[20] I. Buttinoni, J. Bialké, F. Kümmel, H. Löwen, C. Bechinger, and T. Speck, Phys. Rev. Lett. **110**, 238301 (2013).
[21] F. Ginot, I. Theurkauff, F. Detcheverry, C. Ybert, and C. Cottin-Bizonne, Nat. Comm. **9**, 696 (2018).
[22] D. P. Singh, U. Choudhury, P. Fischer, and A. G. Mark, Advanced Materials **29**.
[23] M. N. van der Linden, L. C. Alexander, D. G. Aarts, and O. Dauchot, Physical review letters **123**, 098001 (2019).
[24] F. Peruani, J. Starruß, V. Jakovljevic, L. Søgaard-Andersen, A. Deutsch, and M. Bär, Phys. Rev. Lett. **108**, 098102 (2012).
[25] A. P. Petroff, X.-L. Wu, and A. Libchaber, Phys. Rev. Lett. **114**, 158102 (2015).
[26] D. Dell'Arciprete, M. Blow, A. Brown, F. Farrell, J. S. Lintuvuori, A. McVey, D. Marenduzzo, and W. C. Poon, Nat. Comm. **9**, 4190 (2018).
[27] L. Caprini, U. M. B. Marconi, and A. Puglisi, Physical Review Letters **124**, 078001 (2020).
[28] L. Caprini, U. M. B. Marconi, C. Maggi, M. Paoluzzi, and A. Puglisi, Physical Review Research **2**, 023321 (2020).
[29] J. Bialké, H. Löwen, and T. Speck, EPL (Europhysics Letters) **103**, 30008 (2013).
[30] T. Speck, The European Physical Journal Special Topics **225**, 2287 (2016).
[31] B. Liebchen and D. Levis, Physical review letters **119**, 058002 (2017).
[32] D. Levis, J. Codina, and I. Pagonabarraga, Soft Matter **13**, 8113 (2017).
[33] A. P. Solon, H. Chaté, and J. Tailleur, Physical review letters **114**, 068101 (2015).
[34] E. Tjhung, C. Nardini, and M. E. Cates, Physical Review X **8**, 031080 (2018).
[35] P. Chiarantoni, F. Cagnetta, F. Corberi, G. Gonnella, and A. Suma, Journal of Physics A: Mathematical and Theoretical (2020).
[36] F. Jose, S. K. Anand, and S. P. Singh, arXiv preprint arXiv:2004.01996 (2020).
[37] S. Mandal, B. Liebchen, and H. Löwen, Physical Review Letters **123**, 228001 (2019).
[38] X.-q. Shi, G. Fausti, H. Chaté, C. Nardini, and A. Solon, arXiv preprint arXiv:2007.03587 (2020).
[39] A. Costanzo, R. Di Leonardo, G. Ruocco, and L. Angelani, Journal of Physics: Condensed Matter **24**, 065101 (2012).
[40] N. Figueroa-Morales, G. L. Mino, A. Rivera, R. Caballero, E. Clément, E. Altshuler, and A. Lindner, Soft matter **11**, 6284 (2015).
[41] Y. Yawata, J. Nguyen, R. Stocker, and R. Rusconi, Journal of bacteriology **198**, 2589 (2016).
[42] J. Simmchen, J. Katuri, W. E. Uspal, M. N. Popescu, M. Tasinkevych, and S. Sánchez, Nature communications **7**, 10598 (2016).
[43] L. Caprini and U. M. B. Marconi, Soft matter **14**, 9044 (2018).
[44] C. Maggi, U. M. B. Marconi, N. Gnan, and R. Di Leonardo, Scientific reports **5**, 10742 (2015).
[45] R. Wittmann and J. M. Brader, EPL (Europhysics Letters) **114**, 68004 (2016).
[46] S. Das, S. Ghosh, and R. Chelakkot, arXiv preprint arXiv:2001.04654 (2020).
[47] H. Wensink and H. Löwen, Physical Review E **78**, 031409 (2008).
[48] V. Khodygo, M. T. Swain, and A. Mughal, Physical Review E **99**, 022602 (2019).
[49] L. Caprini and U. M. B. Marconi, Soft matter **15**, 2627 (2019).
[50] X. Yang, M. L. Manning, and M. C. Marchetti, Soft matter **10**, 6477 (2014).
[51] A. Kudrolli, G. Lumay, D. Volfson, and L. S. Tsimring, Physical review letters **100**, 058001 (2008).
[52] J. Harder, S. Mallory, C. Tung, C. Valeriani, and A. Cacciuto, The Journal of chemical physics **141**, 194901 (2014).
[53] D. Ray, C. Reichhardt, and C. O. Reichhardt, Physical Review E **90**, 013019 (2014).
[54] R. Ni, M. A. C. Stuart, and P. G. Bolhuis, Physical review letters **114**, 018302 (2015).
[55] M. Knežević and H. Stark, EPL (Europhysics Letters) **128**, 40008 (2020).

[56] M. L. Kilfoil, E. E. Pashkovski, J. A. Masters, and D. Weitz, Philosophical Transactions of the Royal Society of London. Series A: Mathematical, Physical and Engineering Sciences **361**, 753 (2003).

[57] E. K. Hobbie, Physical review letters **81**, 3996 (1998).

[58] B. Dersoir, A. Schofield, and H. Tabuteau, Soft matter **13**, 2054 (2017).

[59] A. Sauret, K. Somszor, E. Villermaux, and E. Dressaire, Physical Review Fluids **3**, 104301 (2018).

[60] C. M. Cejas, F. Monti, M. Truchet, J.-P. Burnouf, and P. Tabeling, Physical Review E **98**, 062606 (2018).

[61] S. Pal and A. A. Kulkarni, Chemical Engineering Science **199**, 88 (2019).

[62] É. Fodor and M. C. Marchetti, Physica A: Statistical Mechanics and its Applications **504**, 106 (2018).

[63] M. R. Shaebani, A. Wysocki, R. G. Winkler, G. Gompper, and H. Rieger, Nature Reviews Physics , 1 (2020).

[64] G. S. Redner, M. F. Hagan, and A. Baskaran, Phys. Rev. Lett. **110**, 055701 (2013).

[65] A. P. Solon, J. Stenhammar, M. E. Cates, Y. Kafri, and J. Tailleur, New Journal of Physics **20**, 075001 (2018).

[66] P. Digregorio, D. Levis, A. Suma, L. F. Cugliandolo, G. Gonnella, and I. Pagonabarraga, Physical review letters **121**, 098003 (2018).

[67] I. Petrelli, P. Digregorio, L. F. Cugliandolo, G. Gonnella, and A. Suma, The European Physical Journal E **41**, 128 (2018).

[68] N. Nikola, A. P. Solon, Y. Kafri, M. Kardar, J. Tailleur, and R. Voituriez, Physical review letters **117**, 098001 (2016).

[69] F. Smallenburg and H. Löwen, Physical Review E **92**, 032304 (2015).

[70] A. Wysocki, J. Elgeti, and G. Gompper, Physical Review E **91**, 050302 (2015).

[71] J.-C. Wu, K. Lv, W.-W. Zhao, and B.-Q. Ai, Chaos: An Interdisciplinary Journal of Nonlinear Science **28**, 123102 (2018).

[72] L. Caprini, F. Cecconi, and U. Marini Bettolo Marconi, The Journal of chemical physics **150**, 144903 (2019).

[73] S.-j. Shi, H.-s. Li, G. Feng, K. Chen, *et al.*, Physical Chemistry Chemical Physics (2020).

[74] A. Kaiser, H. Wensink, and H. Löwen, Physical review letters **108**, 268307 (2012).

[75] M. Mijalkov and G. Volpe, Soft Matter **9**, 6376 (2013).

[76] N. Kumar, R. K. Gupta, H. Soni, S. Ramaswamy, and A. Sood, Physical Review E **99**, 032605 (2019).